Supporting information

Nonadiabatic *ab initio* chemical reaction dynamics on photoisomerization reaction of 3,5-dimethylisoxazole via the S_1 electronic state

Mizuki Kimura[a] and Shinkoh Nanbu*[b]

[a] Graduate School of Science and Technology, Sophia University, Japan, Chiyoda, Tokyo 102-8554, Japan. Email: m-kimura-0o3@eagle.sophia.ac.jp

[b] Faculty of Science and Technology, Sophia University, Chiyoda, Tokyo 102-8554, Japan

3,5-dimethylisoxazole cartesian coordinates (Å) at XMS-CASPT2

C	-1.0807968992	-0.1539346183	0.0000413499
O	-0.6956793940	1.1154687627	0.0002126342
C	1.1180432032	-0.0835435722	0.0000418655
C	0.0072335861	-0.9700101663	-0.0000731874
H	0.0119141080	-2.0458347911	-0.0002195165
N	0.7068855225	1.1861933694	0.0002178806
C	2.5800859095	-0.4061675012	-0.0000002889
H	2.8465515175	-0.9892996825	-0.8830950506
H	3.1666385010	0.5109069911	0.0001125293
H	2.8465596987	-0.9895446218	0.8829170534
C	-2.5518274005	-0.4113644303	0.0000114633
H	-3.0177176837	0.0253751514	-0.8834620528
H	-2.7411160110	-1.4837469412	-0.0001352872
H	-3.0177110631	0.0251321742	0.8836085392

3,5-dimethylisoxazole cartesian coordinates (Å) at SA4-CASSCF

C	-1.0837935534	-0.1563189470	0.0000407423
O	-0.6996231333	1.1212286737	0.0002126098
C	1.1211549246	-0.0802075405	0.0000418025
C	0.0062327251	-0.9709083766	-0.0000737954
H	0.0171859222	-2.0466641533	-0.0002198474
N	0.7127128686	1.1876898265	0.0002184199
C	2.5828337652	-0.4058281698	-0.0000008999
H	2.8459517777	-0.9904278277	-0.8830628445
H	3.1727419093	0.5091853677	0.0001148214
H	2.8459583901	-0.9906763671	0.8828830206
C	-2.5547245554	-0.4114151366	0.0000118302
H	-3.0219810679	0.0242015854	-0.8834272549
H	-2.7436120934	-1.4841907225	-0.0001328988
H	-3.0219742844	0.0239619114	0.8835722108

Table S1(a) The primary CSF for each state and the squared values of transition dipole moment (TDM) at SA4-CASSCF

Electronic State	Primary Electronic Configuration	TDM^2 / a_0^2
S_1	$Ryd \leftarrow (\pi_{NO} + \pi_{CCC})^*$	0.119
S_2	$\pi_{NC}^* + \pi_{OC}^* \leftarrow (\pi_{NO} + \pi_{CCC})^*$	0.437
S_3	$\pi_{NC}^* + \pi_{OC}^* \leftarrow (n_N + \sigma_{CO+CC})^*$	0.111

Table S1(b) The vertical excitation energy (E_h)

Electronic State	XMS-CASPT2/ cc-pVDZ + sp	SA4-CASSCF/ cc-pVDZ + sp	SAC-CI/ aug-cc-pVDZ	SAC-CI/ cc-pVTZ
S_0	-323.01051634	-323.53623696	-323.262988	-323.375982
S_1	-322.77050436	-323.28875461	-323.032850	-323.128486
S_2	-322.76137757	-323.28280562	-323.024065	-323.120191
S_3	-322.74817739	-323.26228710	-323.007678	-323.087671

21a   22a   23a   24a   25a   26a

$(\pi_{CO} + \pi_{CCN})^*$ $(n_N + \sigma_{CO+CC})^*$ $(\pi_{NO} + \pi_{CCC})^*$

27a   28a   29a   30a   31a

$(\pi_{NC}^* + \pi_{CO}^*)^*$ *Rydberg* orbital around C5 carbon $(\pi_{NO} + \pi_{CCC}^*)^*$
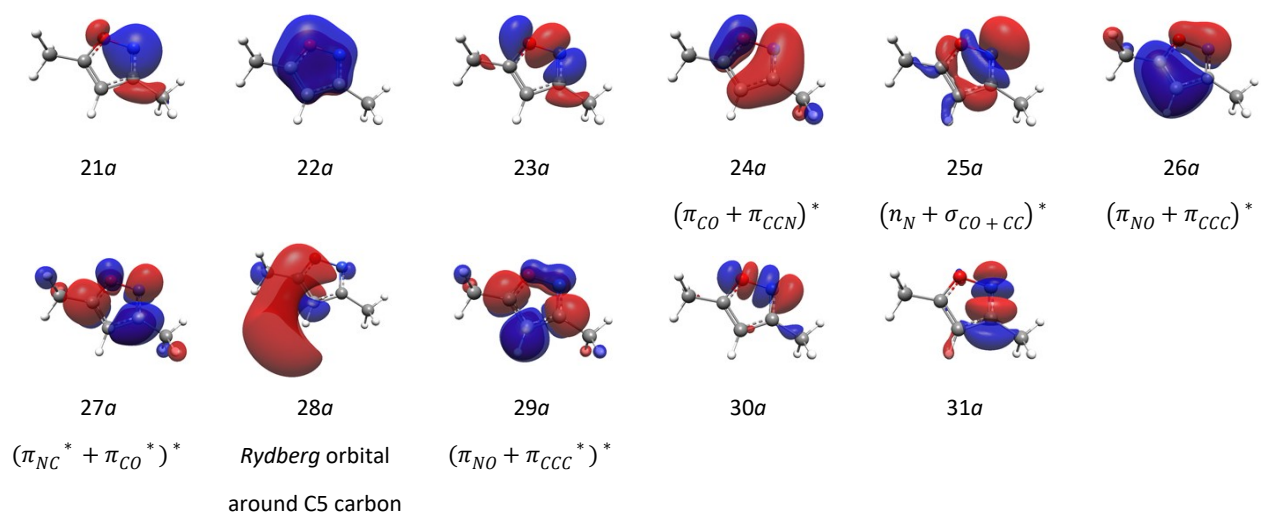
Fig. S1 The molecular orbitals (MOs) in the active space for SA4-CASSCF

Table S2(a) The coefficients of the correlation interaction (CI) for the S_0, S_1, S_2, and S_3 states at XMS-CASPT2 level

Configuration State Function (CSF)	S_0	S_1	S_2	S_3
$(24a)^2(25a)^2(26a)^2(27a)^0(28a)^0(29a)^0$	-0.9387224	0.0000001	-0.0000204	-0.0433679
$(24a)^2(25a)^2(26a)^1(27a)^0(28a)^1(29a)^0$	-0.0000001	0.9269819	0.0040877	-0.0000004
$(24a)^2(25a)^2(26a)^1(27a)^1(28a)^0(29a)^0$	0.0000002	0.0041877	0.9149561	-0.0004300
$(24a)^1(25a)^2(26a)^1(27a)^1(28a)^0(29a)^0$	0.0866112	0.0000018	-0.0003280	-0.6938881
$(24a)^1(25a)^2(26a)^2(27a)^0(28a)^0(29a)^1$	0.0550695	0.0000005	0.0001656	0.3500992
$(24a)^2(25a)^2(26a)^0(27a)^1(28a)^0(29a)^1$	-0.0300139	-0.0000000	0.0001544	0.3331554

Table S2(b) The CI coefficients for each electronic state at SA4-CASSCF level

Configuration State Function (CSF)	S_0	S_1	S_2	S_3
$(24a)^2(25a)^2(26a)^2(27a)^0(28a)^0(29a)^0$	-0.9383068	0.0000001	-0.0439348	0.0000123
$(24a)^2(25a)^2(26a)^1(27a)^0(28a)^1(29a)^0$	-0.0000003	0.9267115	0.0000040	0.0034411
$(24a)^2(25a)^2(26a)^1(27a)^1(28a)^0(29a)^0$	0.0850873	0.0000037	-0.7063145	0.0001956
$(24a)^1(25a)^2(26a)^2(27a)^1(28a)^0(29a)^0$	0.0562196	0.0000008	0.3372313	-0.0000930
$(24a)^1(25a)^2(26a)^2(27a)^0(28a)^0(29a)^1$	-0.0307454	-0.0000003	0.3273773	-0.0000958
$(24a)^2(25a)^1(26a)^2(27a)^1(28a)^0(29a)^0$	0.0000003	0.0043313	0.0002571	0.9139180

Table S3 (a) The first peak of the histogram of distance in comparison by brute force of structures with non-adiabatic transitions
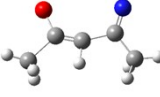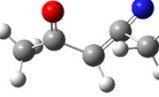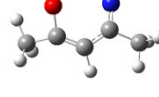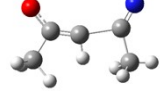
(id, Time / fs)	Distance, d	Probability, p	Geometry1	Geometry2
(021, 74.75), (495, 114.25)	3.24	0.92, 0.88		
(133, 77.75), (385, 372.00)	3.19	1.00, 0.92		
(159, 50.00), (531, 128.00)	3.24	1.00, 0.99		
(397, 55.00), (487, 512)	3.24	0.96, 0.96		
(417, 82.00), (495, 114.25)	3.15	1.00, 0.88		

Table S3 (b)The second peak of the histogram of distance in comparison by brute force of structures with non-adiabatic transitions
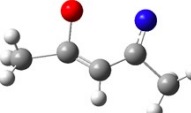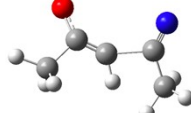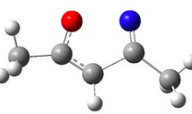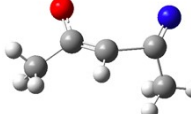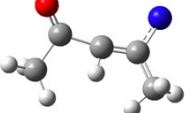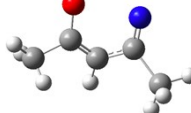
(id, Time / fs)	Distance, d	Probability, p	Geometry1	Geometry2
(105, 343.50), (257, 71.75)	6.62	0.97, 0.68		
(151, 26.00), (403, 127.75)	6.62	0.97, 0.87		
(181, 53.50), (293, 77.25)	6.61	0.88, 0.84		
(263, 216.75), (429, 138.50)	6.63	0.97, 0.92		
(443, 87.00), (595, 261.50)	6.67	0.29, 0.93		

Table S4 (a)The primary peak around d=18.03
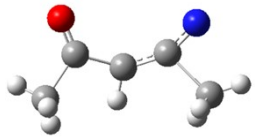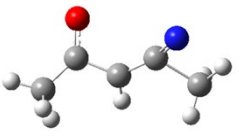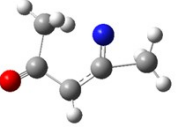
(id, Time / fs)	Distance, d	Probability, p	Geometry
(021, 132.75)	18.15	0.54	
(095, 67.75)	18.21	0.98	
(185, 320.00)	18.17	0.61	
(203, 64.00)	17.90	0.96	
(231, 413.00)	18.06	0.98	

Table S4 (b) The subsidiary peak around d = 9.98
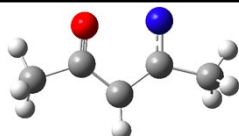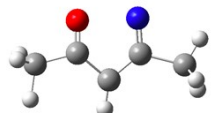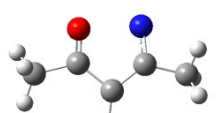
(id, Time / fs)	Distance, d	Probability, p	Geometry
(011, 24.00)	9.98	0.84	
(349, 21.25)	9.91	0.95	
(145, 25.00)	10.07	0.54	
(157, 18.00)	9.87	1.00	
(519, 19.75)	10.09	0.98	

Table S4 (c) Time-resolved histograms.

Time / fs	Distance, *d*	Time / fs	Distance, *d*
0 ~ 50	Histogram of Distance	250 ~ 300	Histogram of Distance
50 ~ 100	Histogram of Distance	300 ~ 350	Histogram of Distance
100 ~ 150	Histogram of Distance	350 ~ 400	Histogram of Distance
150 ~ 200	Histogram of Distance	400 ~ 500	Histogram of Distance
200 ~ 250	Histogram of Distance		
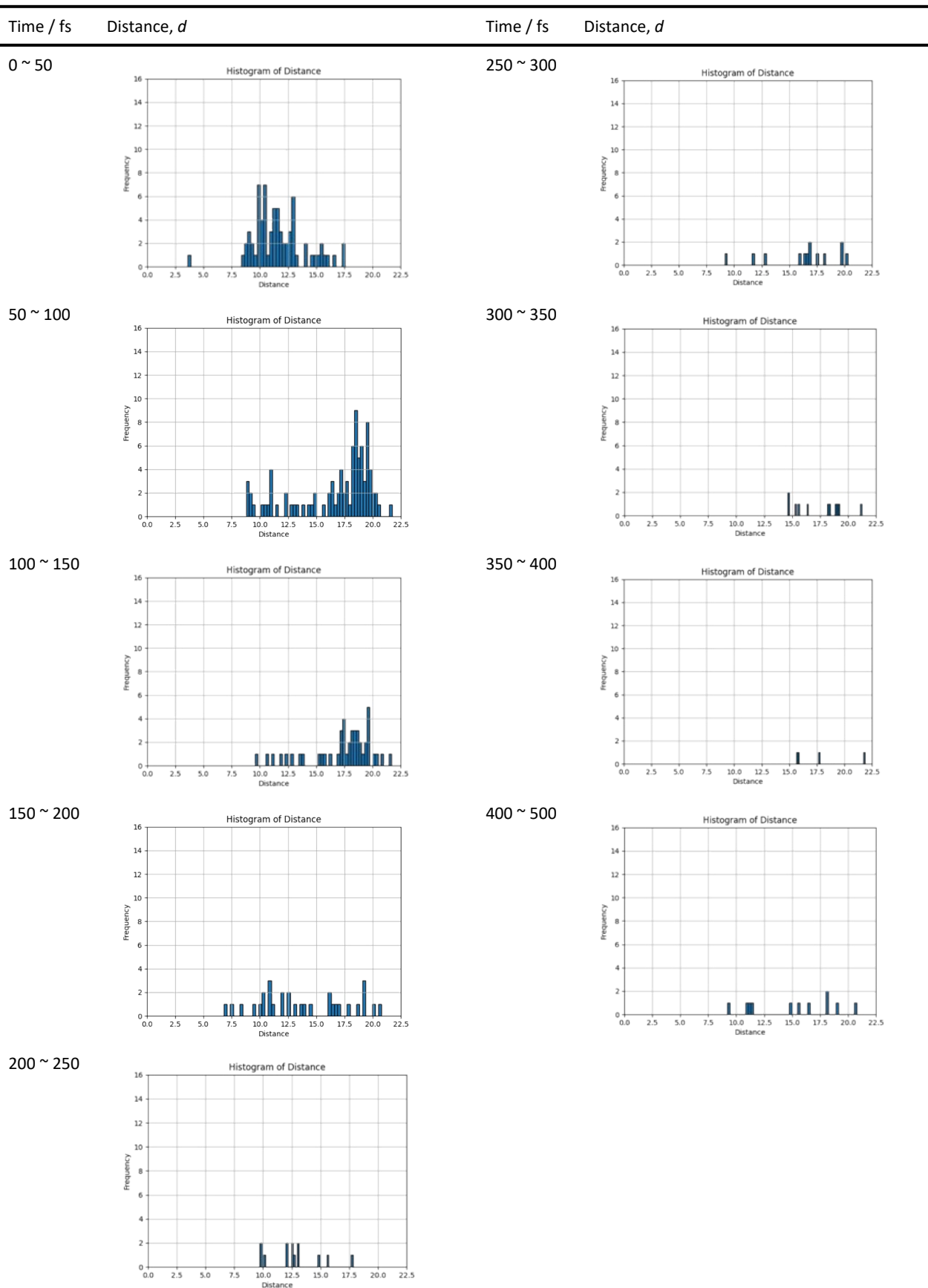
(a)
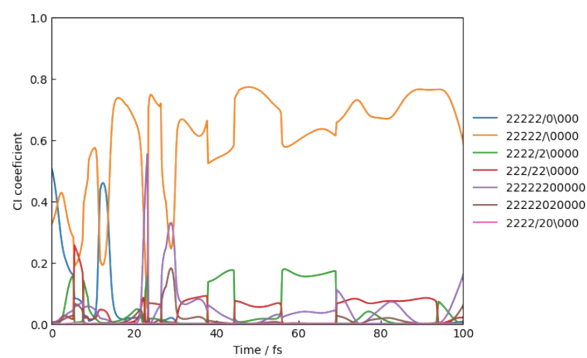
(b)
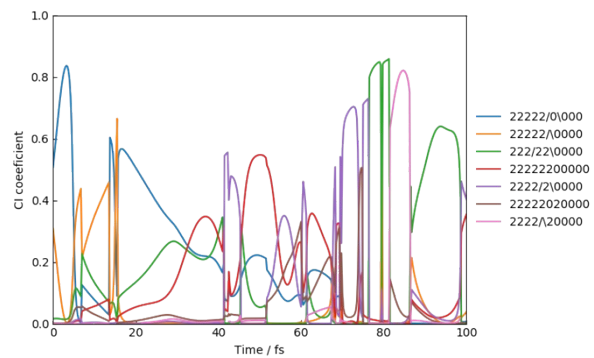
Fig. S2 (a) and (b) are time variations of the CI-coefficients between 100 fs corresponding to Figures 6(b) and 6(d).

Table S5 (a) The time variation for molecular orbitals on the trajectory producing azirine after photoexcitation
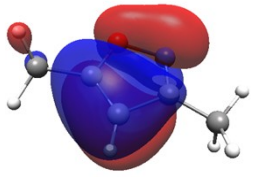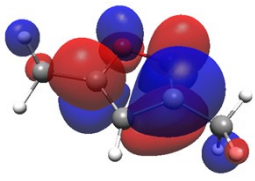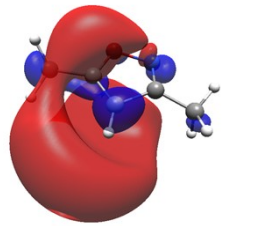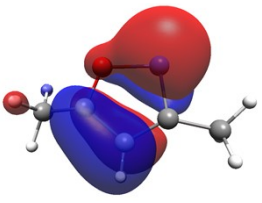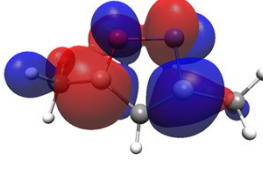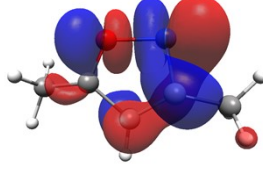
Time / fs	26*a*	27*a*	28*a*
0.00			
10.0			

Table S5(b) The time variation for molecular orbitals on the trajectory producing azirine
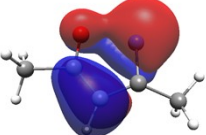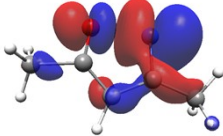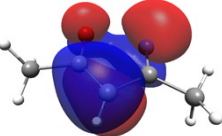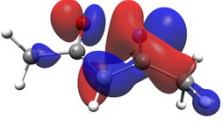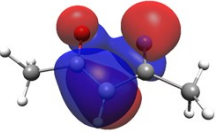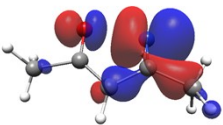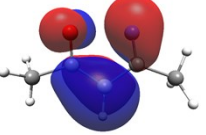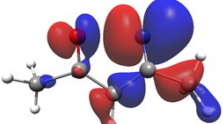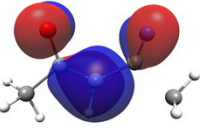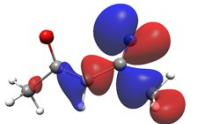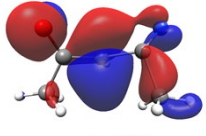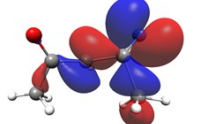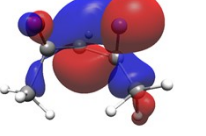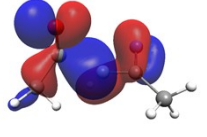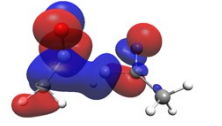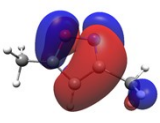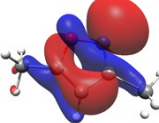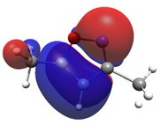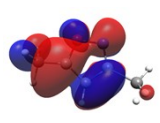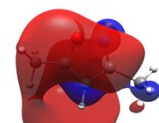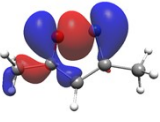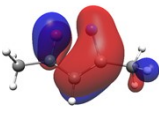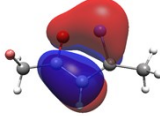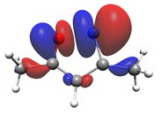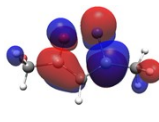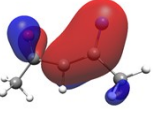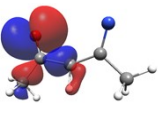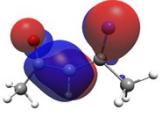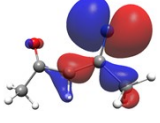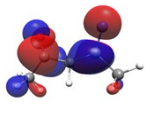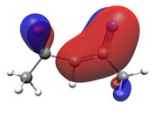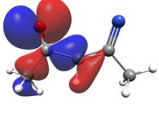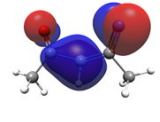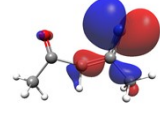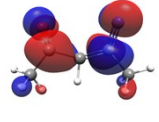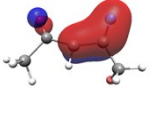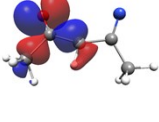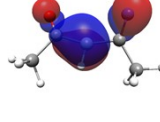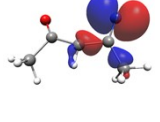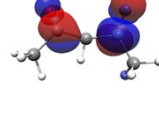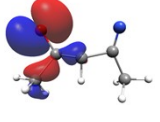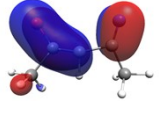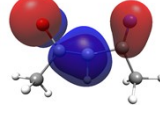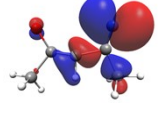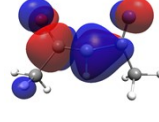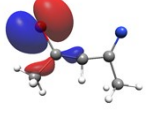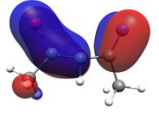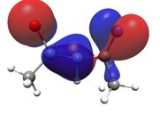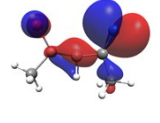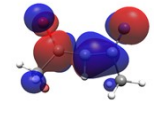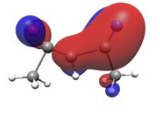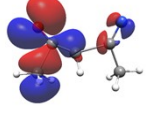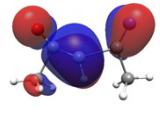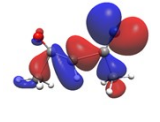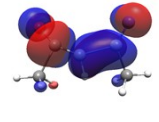
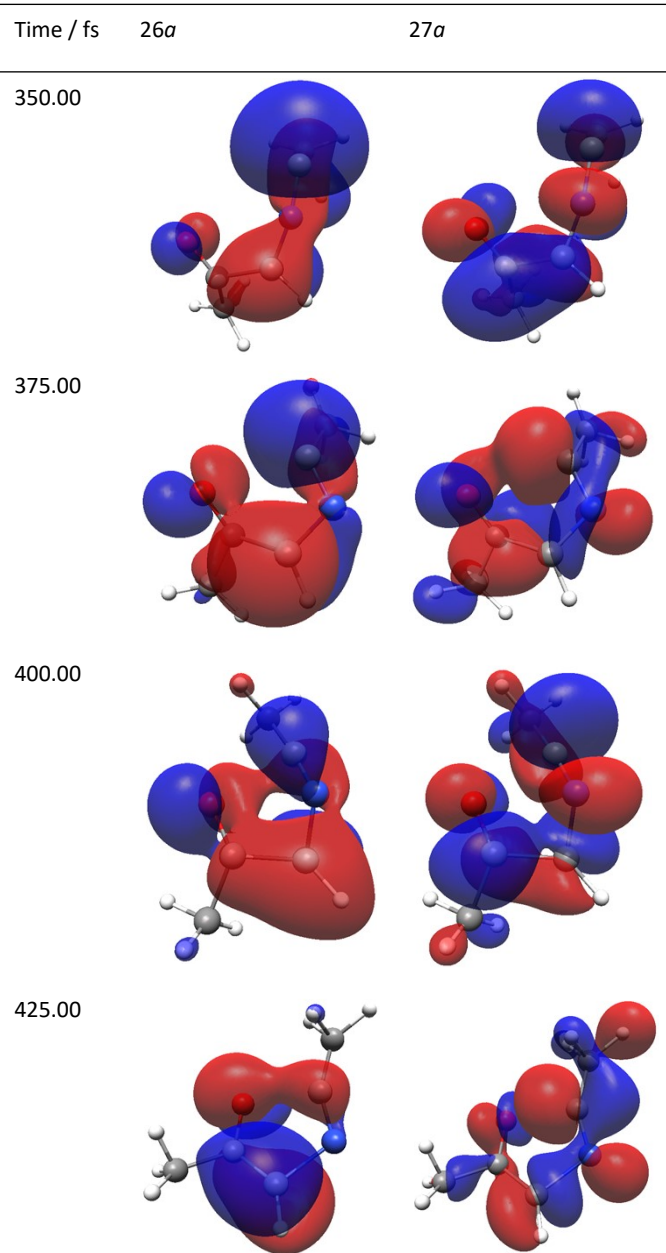| Time / fs	26*a*	27*a*
18.75		
22.50		
23.50		
25.00		
50.00		
100.00		
150.00		
250.00		

Table S5(c) The time variation for molecular orbitals on the trajectory producing azirine after photoexcitation

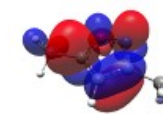| Time / fs	24*a*	25*a*	26*a*	27*a*	28*a*
0.00					
15.50					
68.25					
69.75					
74.75					
79.50					
86.50					
104.75					

(a)
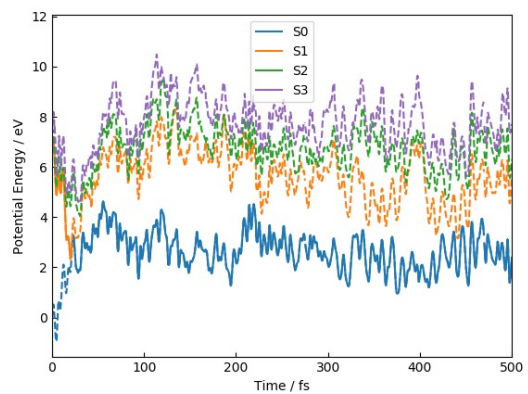
(b)
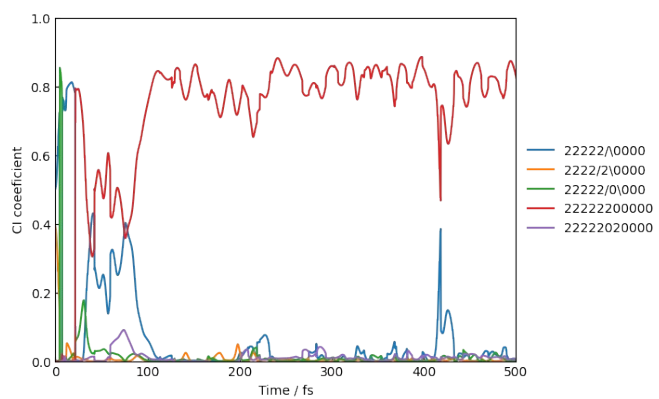
Fig. S3 The isomerization pathways to nitrile ylide product at XMS-CASPT2 level: (a) the potential energies of four electronic states over the time evolution, and (b) CI coefficients over the same time are shown. The legends used in (b) is mentioned in **Fig. 6**.

Table S6(a) The time variation for molecular orbitals on the trajectory producing nitrile ylide and oxazole
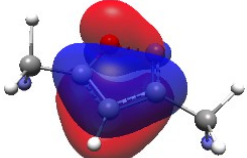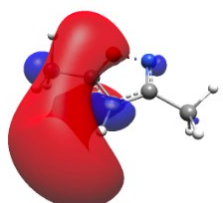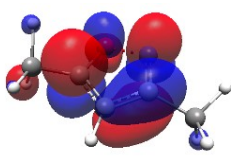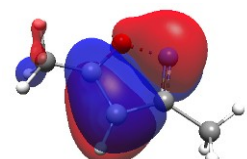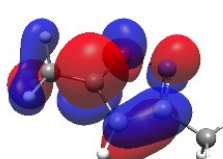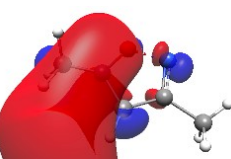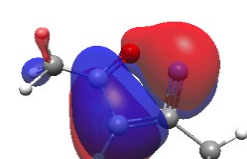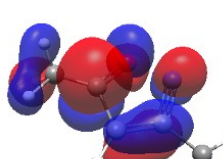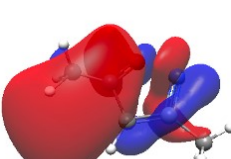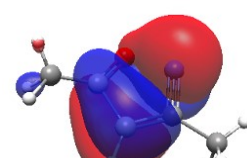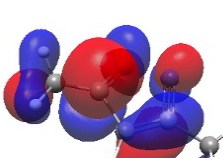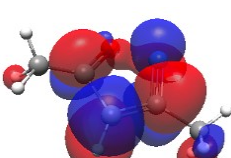
Time / fs	26*a*	27*a*	28*a*
0.00			
4.75			
7.25			
7.50			

Table S6(b) The time variation for molecular orbitals on the trajectory producing nitrile ylide and oxazole
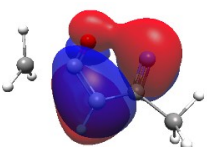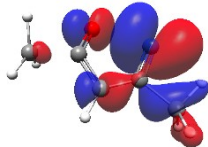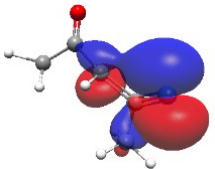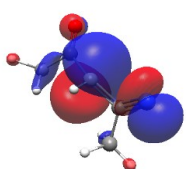
Time / fs	26*a*	27*a*
21.50		
76.00		

Table S6(c) The time variation for molecular orbitals on the trajectory producing nitrile ylide
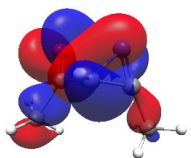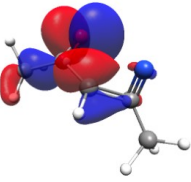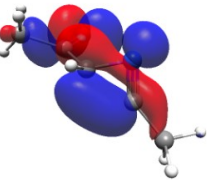
Time / fs	26*a*
150.00	
175.00	
200.00	

Table S6(d) The time variation for molecular orbitals on the trajectory producing oxazole

Time / fs	26*a*	27*a*
350.00		
375.00		
400.00		
425.00		

Table S7(a) The time variation for molecular orbitals on the trajectory producing ketenimine
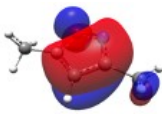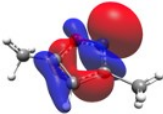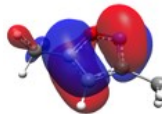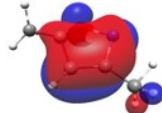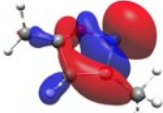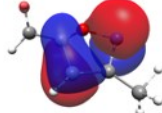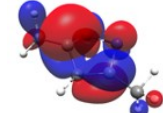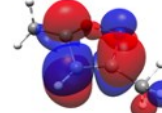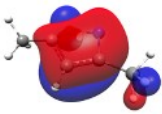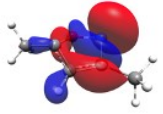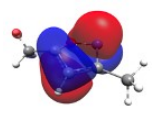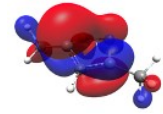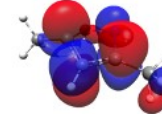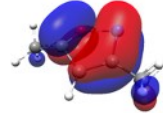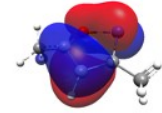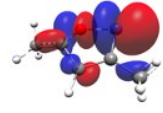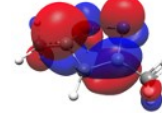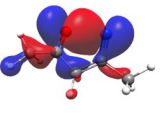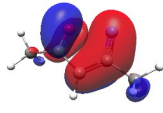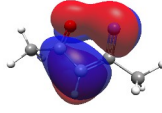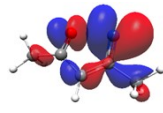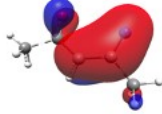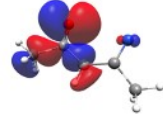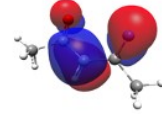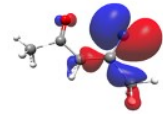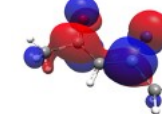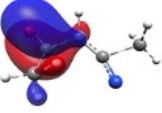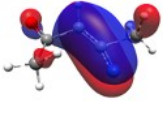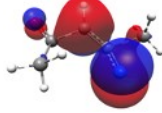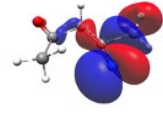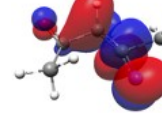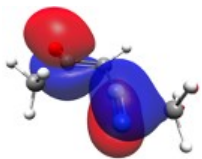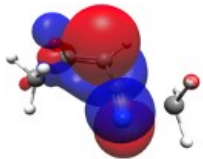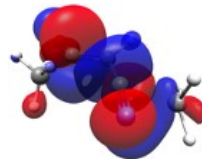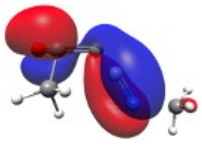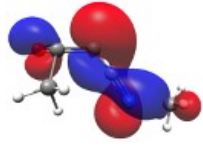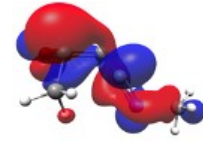
Time/ fs	24*a*	25*a*	26*a*	27*a*	28*a*
0.00					
16.75					
28.25					
55.75					
65.00					
92.50					
361.75					

Table S7(b) The time variation for molecular orbitals on the trajectory migrating the methyl group.

Time / fs	25a	26a	27a	28a
375.00				
400.00				

(a)

(b)

26*a*   27*a*   28*a*

(c)

4*a*   10*a*   15*a*   17*a*   24*a*
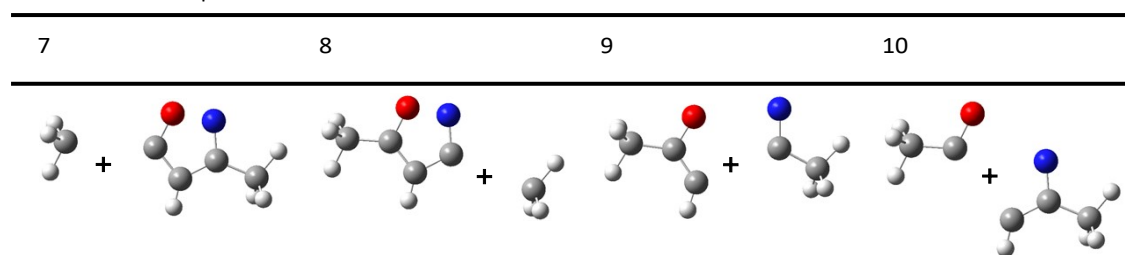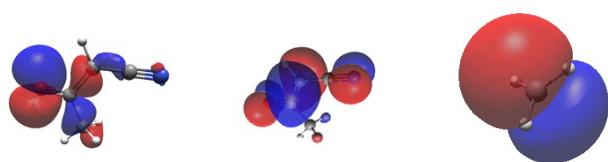
(d)

1*a*   2*a*   3*a*   4*a*   5*a*

Fig. S4 The methyl shift, (a) the optimized geometry of conical intersection, (b) MOs at the optimized conical intersection, (c) MOs for the methyl migration in our trajectory, and (d) MOs for methyl radical only
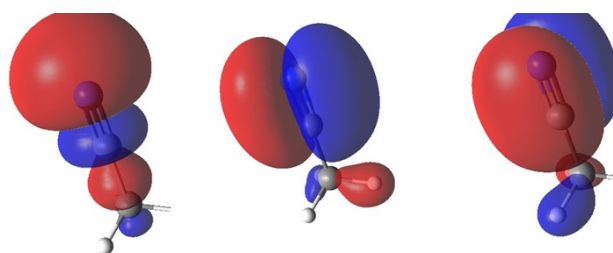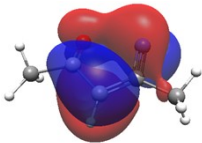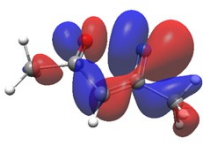
Table S8 The other products

7	8	9	10

(a)

25*a*   26*a*   27*a*

(b)

23*a*   26*a*

(c)
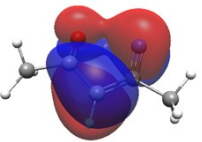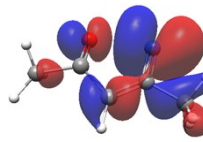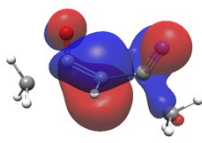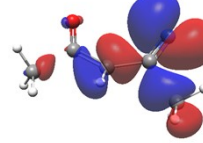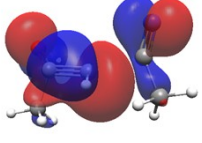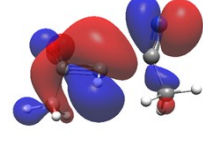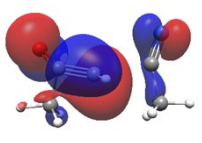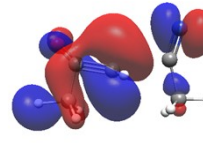
9*a*   10*a*   11*a* HOMO

Fig. S5 The molecular orbitals for the other products for (a) the C3-C7 bond dissociation, (b) $CH_3CN + CH_3CCO$, and (c) CH_3CN
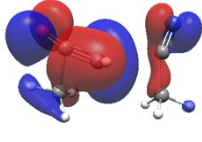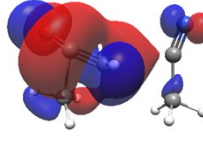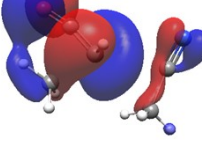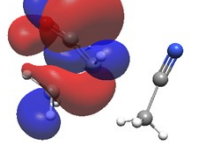
Table S9 The time variation of molecular orbitals for producing acetonitrile and 1,2 -shift

Time / fs	26*a*	27*a*
24.00		
25.00		
50.00		
75.00		
81.25		
87.50		
93.75		
100.00		